Supplement of Atmos. Chem. Phys., 24, 9923–9937, 2024
https://doi.org/10.5194/acp-24-9923-2024-supplement

Atmospheric Chemistry and Physics
Open Access
EGU

Supplement of

Global assessment of climatic responses to ozone–vegetation interactions

Xinyi Zhou et al.

Correspondence to: Xu Yue (yuexu@nuist.edu.cn)

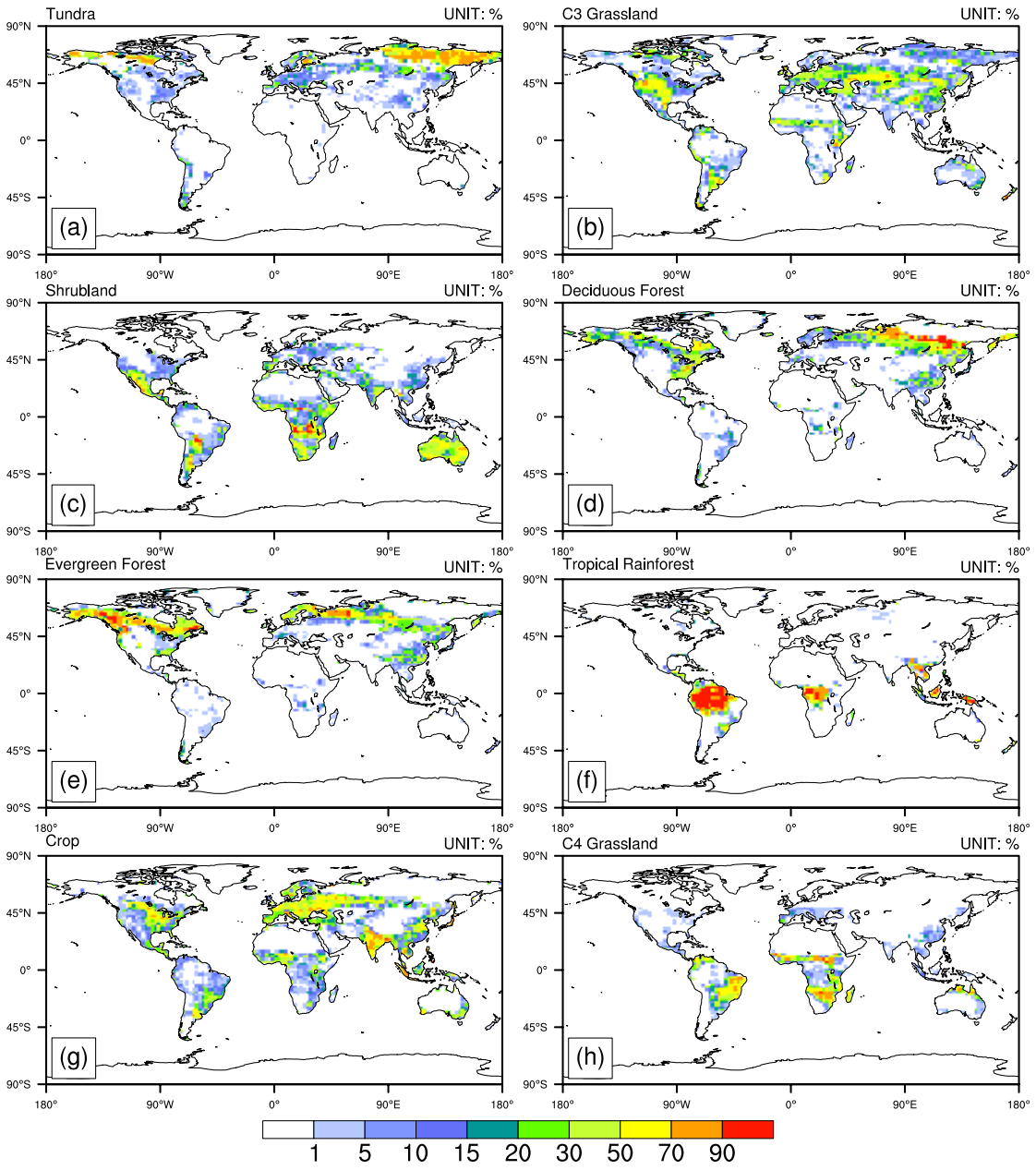

Fig. S1. The cover fraction of 8 plant functional types (PFTs) from the LUH2 used in the ModelE2-YIBs model.

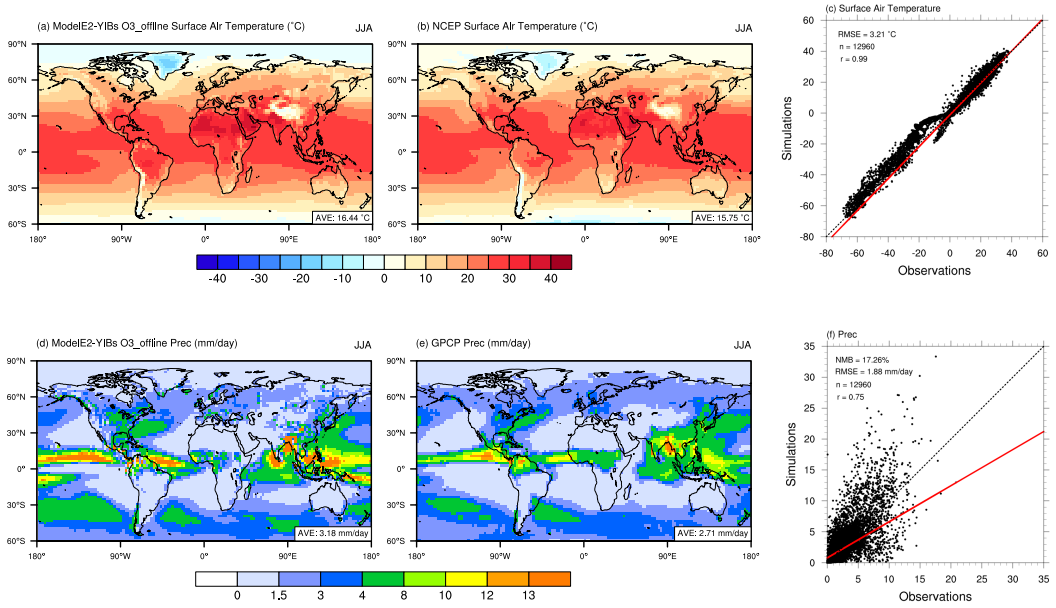

Fig. S2. Evaluation of the present-day boreal summertime (June–August) meteorological field simulated by the ModelE2-YIBs model. Surface air temperature (a-c) and precipitation (d-f) from the simulation O3_offline (a & d) and reanalysis data (b & e) are compared. The correlation coefficient (r), root mean square error (RMSE), normalized mean bias (NMB), and number of grid cells (n) for the comparisons are calculated between the simulations and observations are listed on the scatter panels.

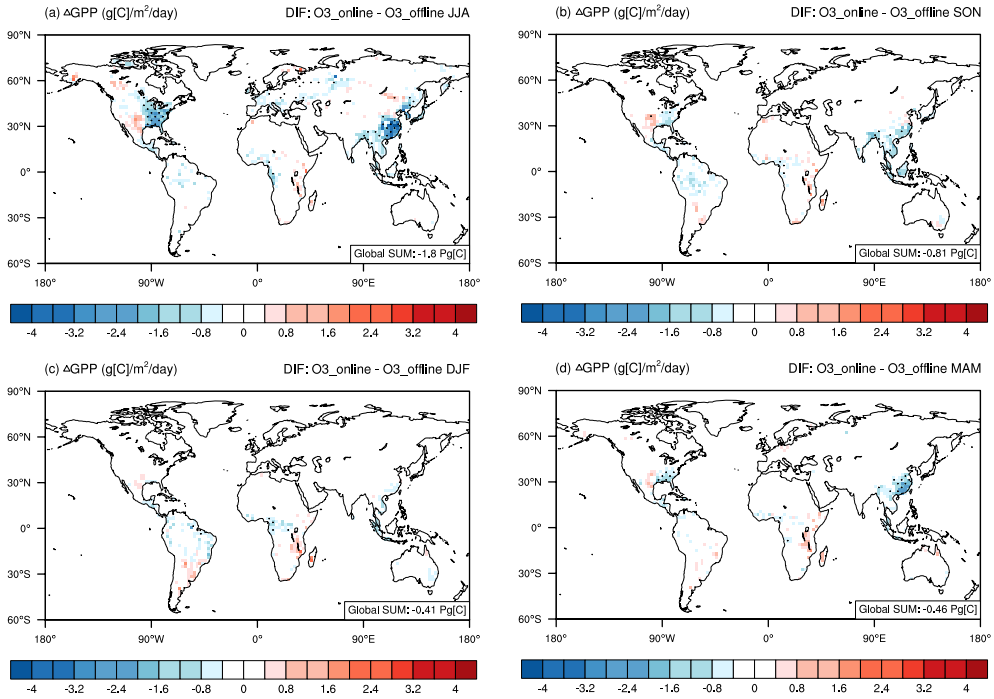

Fig. S3. Changes in present-day GPP in different seasons caused by O_3–vegetation interactions. The results shown are changes in (a) JJA (June-July-August), (b) SON (September-October-November), (c) DJF (December-January-Feburary), and (d) MAM (March-April-May) between the O3_online and O3_offline simulations. The black dots denote areas with significant changes ($p < 0.1$).

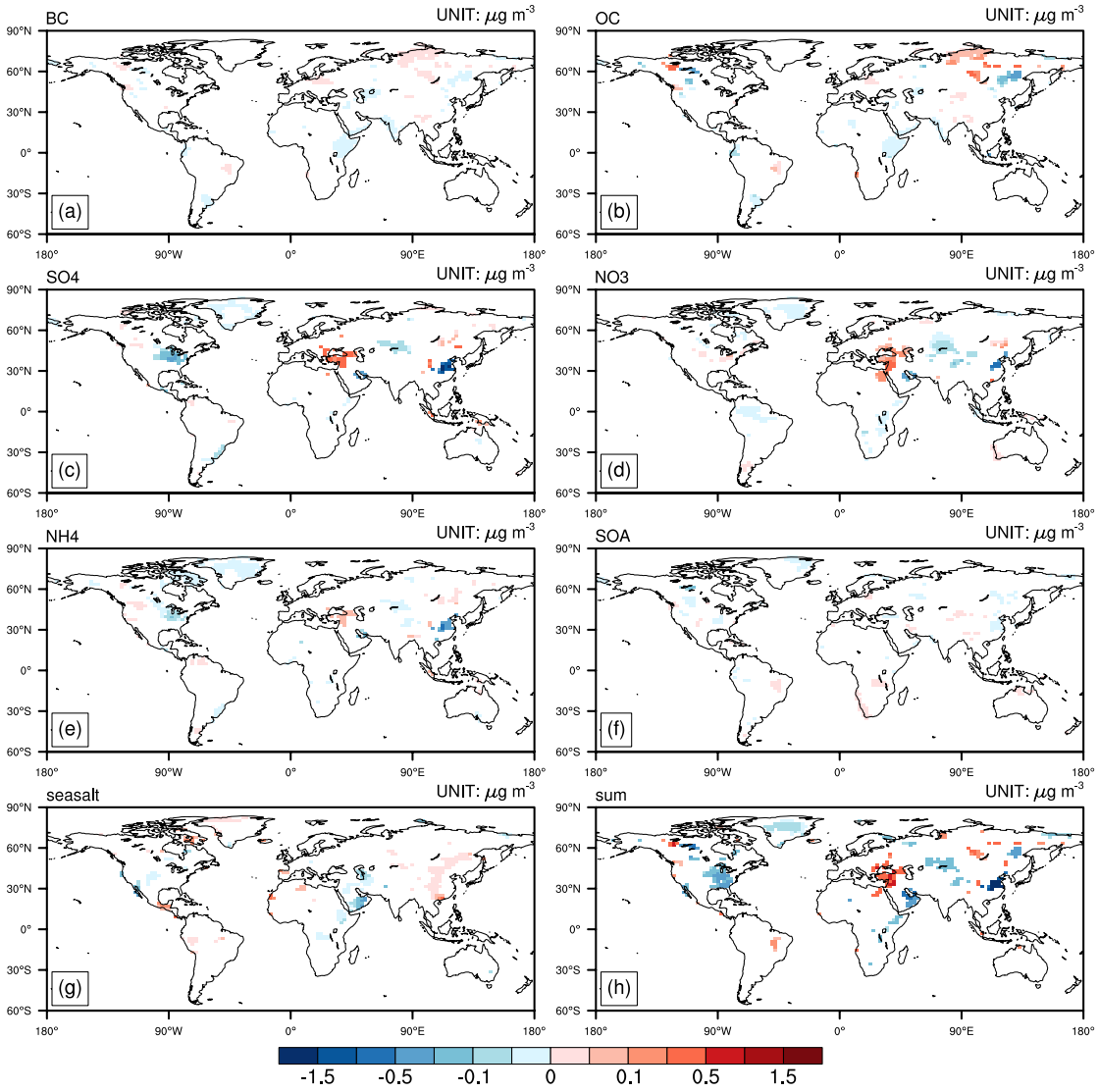

Fig. S4. Changes in present-day summertime 7 types (a-g) $PM_{2.5}$ (without silts) and their sum (h) caused by O_3–vegetation interactions. The results shown are changes in $PM_{2.5}$ between the O3_online and O3_offline simulations. Only the significant changes ($p < 0.1$) are presented.

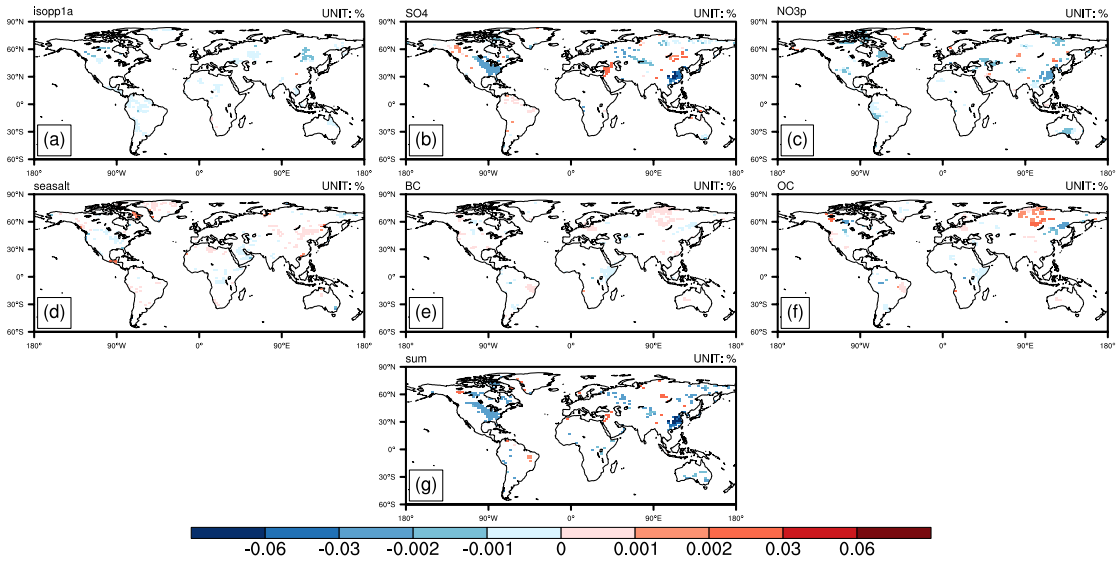

Fig. S5. Changes in present-day summertime 6 types (a-f) AOD and their sum (g) caused by O_3–vegetation interactions. The results shown are changes in AOD between the O3_online and O3_offline simulations. Only the significant changes ($p < 0.1$) are presented.

Table S1. Parameters for O_3 damage scheme

PFT[a]	TDA	CRAC3	CRAC4	SHR	DBF	ENF	TRF	CRO	
Carboxylation	C_3	C_3	C_4	C_3	C_3	C_3	C_3	C_3	C_4
$F_{O3,crit}$ (nmol m^{-2} s^{-1})	1.6	5	5	1.6	1.6	1.6	1.6	5	5
a_h [b] (mmol m^{-2})	0.1	1.4	0.735	0.1	0.15	0.075	0.15	1.4	0.735

[a] Plant function types (PFTs) are tundra (TDA), C_3 grassland (GRAC3), C_4 savanna/grassland (GRAC4), shrubland (SHR), deciduous broadleaf forest (DBF), evergreen needleleaf forest (ENF), tropical rainforest (TRF), and cropland (CRO).

[b] Parameters a_h is the high O_3-damaging sensitivities.

Table S2. Relative changes of terrestrial ecosystems in two major geographic regions in response to O_3-vegetation interactions in model

Region	GPP	Stomatal Conductance	LAI
eastern China	-25.40±1.90%	-30.62±4.30%	-4.53±1.14%
eastern U.S.	-20.14±5.02%	-25.65±9.32%	-5.87±3.11%

Table S3. Changes of climatic variables in two major geographic regions in response to O_3-vegetation interactions in model

Region	Surface Air Temperature (unit: °C)	Precipitation (unit: mm day^{-1})	Sensible Heat Flux ($W\ m^{-2}$)
eastern China	0.56±0.38°C	-0.79±1.05 (16.18±20.38%)	7.12±3.86 (25.46±14.71%)
eastern U.S.	0.33±0.87 °C	-0.45±1.33 (-9.82±14.20%)	6.3±5.4 (16.54±15.59%)

Table S4. Changes of air pollution in two major geographic regions in response to O_3-vegetation interactions in model

Region	MDA8 O_3 (ppbv)	$PM_{2.5}$ (unit: μg m^{-3})	AOD
eastern China	1.46±3.02	-1.94±1.67	-0.06±0.05
		(-8.52±6.88%)	(-14.67±16.75%)
eastern U.S.	1.15±1.77	-0.27±0.36	-0.01±0.01
		(-6.01±7.9%)	(-8.15±9.38%)